Tectonophysics 464 (2009) 10–20

Contents lists available at ScienceDirect

Tectonophysics

journal homepage: www.elsevier.com/locate/tecto

Neogene kinematic history of Nazca–Antarctic–Phoenix slab windows beneath Patagonia and the Antarctic Peninsula

Katrin Breitsprecher [a,*], Derek J. Thorkelson [b]

[a] Department of Earth and Ocean Sciences, University of British Columbia, Vancouver, British Columbia, Canada V6T 1Z4
[b] Department of Earth Sciences, Simon Fraser University, Burnaby, British Columbia, Canada V5A 1S6

ARTICLE INFO

Article history:
Received 13 May 2007
Received in revised form 21 February 2008
Accepted 27 February 2008
Available online 18 March 2008

Keywords:
Ridge subduction
Quadruple junction
Trench–ridge–trench junction
Scotia Basin
Heat flow
Mantle upwelling

ABSTRACT

The Patagonian slab window is a subsurface tectonic feature resulting from subduction of the Nazca–Antarctic spreading-ridge system (Chile Rise) beneath southern South America. The geometry of the slab window had not been rigorously defined, in part because of the complex nature of the history of ridge subduction in the southeast Pacific region, which includes four interrelated spreading-ridge systems since 20 Ma: first, the Nazca–Phoenix ridge beneath South America, then simultaneous subduction of the Nazca–Antarctic and the northern Phoenix–Antarctic spreading-ridge systems beneath South America, and the southern Phoenix–Antarctic spreading-ridge system beneath Antarctica. Spreading-ridge paleo-geographies and rotation poles for all relevant plate pairs (Nazca, Phoenix, Antarctic, South America) are available from 20 Ma onward, and form the mathematical basis of our kinematic reconstruction of the geometry of the Patagonia and Antarctic slab windows through Neogene time. At approximately 18 Ma, the Nazca–Phoenix–Antarctic oceanic (ridge–ridge–ridge) triple junction enters the South American trench; we recognize this condition as an *unstable quadruple junction*. Heat flow at this junction and for some distance beneath the forearc would be considerably higher than is generally recognized in cases of ridge subduction. From 16 Ma onward, the geometry of the Patagonia slab window developed from the subduction of the trailing arms of the former oceanic triple junction. The majority of the slab window's areal extent and geometry is controlled by the highly oblique (near-parallel) subduction angle of the Nazca–Antarctic ridge system, and by the high contrast in relative convergence rates between these two plates relative to South America. The very slow convergence rate of the Antarctic slab is manifested by the shallow levels achieved by the slab edge (<45 km); thus no point on the Antarctic slab is sufficiently deep to generate "normal" mantle-derived arc-type magmas. Upwelling beneath the region may have contributed to uplift and eastward transfer of extension in the Scotia Sea.

1. Introduction

The Patagonian and Antarctic slab windows were produced by Late Cenozoic subduction of the Nazca–Antarctic and Phoenix–Antarctic spreading-ridges, respectively (Forsythe and Nelson, 1985; Hole, 1988). These windows – which are gaps in an otherwise continuous slab of subducting oceanic crust in the region – have been linked to a variety of magmatic processes in southern South America and the Antarctic Peninsula, including (1) an interruption of normal calc-alkaline arc volcanism, and (2) widespread eruption of "anomalous" igneous rocks including alkalic plateau lavas and adakitic volcanoes (e.g., Forsythe et al., 1986; Kay et al., 1993; Hole and Larter, 1993; Gorring et al., 1997; D'Orazio et al., 2001; Gorring and Kay, 2001; Bourgois and Michaud, 2002; Guivel et al., 2003; Lagabrielle et al., 2004; Espinoza et al., 2005; Guivel et al., 2006). This connection between slab windows and anomalous magmatism has been documented in slab windows, both modern and ancient, from numerous worldwide localities (Marshak and Karig, 1977; Dickinson and Snyder, 1979; Johnson and O'Neil, 1984; Forsythe and Nelson, 1985; Staudigel et al., 1987; Hole, 1988; Thorkelson and Taylor, 1989; Gorring et al., 1997; Dickinson, 1997; Johnston and Thorkelson, 1997; Bourgois and Michaud, 2002; Breitsprecher et al., 2003; Groome et al., 2003; Haeussler et al., 2003; Sisson et al., 2003; Wilson et al., 2005; Cole et al., 2006; Madsen et al., 2006).

Despite the importance of slab window formation to the geological evolution of Patagonia and the Antarctic Peninsula, a thorough regional depiction of slab window formation has not been previously carried out. In this paper, we provide an integrated geometrical analysis of Nazca–Antarctica and Antarctica–Phoenix ridge subduction, and show how the Patagonian and Antarctic slab windows developed synchronously to produce a pair of large and persistent slab-free regions in Late Cenozoic time. In the process of our analysis

* Corresponding author. Tel.: +1 778 240 1278; fax: +1 604 822 6088..
E-mail addresses: kbreitsp@eos.ubc.ca (K. Breitsprecher), dthorkel@sfu.ca (D.J. Thorkelson).

0040-1951/$ – see front matter © 2008 Elsevier B.V. All rights reserved.
doi:10.1016/j.tecto.2008.02.013

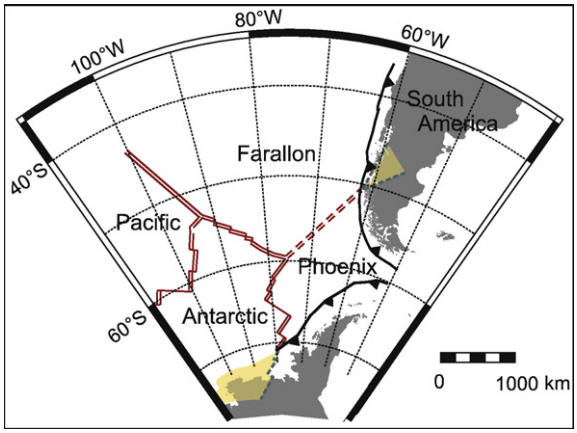

Fig. 1. Possible Eocene configuration of subducting ridges in the southeast Pacific Basin and related slab windows. Plate tectonic models indicate that the Farallon–Phoenix spreading-ridge system intersected the South American trench from Cretaceous to Paleogene time (dashed double red line, e.g. Mayes et al., 1990; Eagles et al., 2004). Note however that both of the triple-junction positions and the configuration and paleo-geometry of the converging spreading-ridge systems are unconstrained by magnetic anomaly data, compared to well-constrained spreading-ridge systems to the south and west (solid red lines). The paleo-position and shape of the concomitant Farallon–Phoenix slab window therefore cannot be constrained. We position the Farallon–Phoenix slab window to coincide with geochemical evidence for it beneath Patagonia of Espinoza et al. (2005), but emphasize the speculative nature of the shape as drawn by the use of dashed lines bounding the slab windows. (For interpretation of the references to colour in this figure legend, the reader is referred to the web version of this article.)

we identify an ephemeral quadruple plate junction that was produced by subduction of an oceanic triple junction (Nazca–Antarctic–Phoenix) beneath the South American plate.

2. Overview: ridge subduction in the southeast Pacific Basin

The Patagonian and Antarctic Peninsulas, situated in the southeastern Pacific Basin, have a long-lived history of ridge subduction involving various pairings of the Pacific, Antarctic, Phoenix (formerly known as the Aluk or Drake), Bellinghausen, Farallon, and Nazca plates. The Pacific–Phoenix spreading-ridge system was subducting beneath the Antarctic Peninsula, and the Farallon–Phoenix spreading-ridge system was subducting beneath Patagonia, as early as the mid-Cretaceous (Barker, 1982; McCarron and Larter, 1998). By the Late Cretaceous, the Pacific–Phoenix spreading-ridge was displaced away from the Antarctic trench by the newly-formed Bellinghausen–Pacific spreading-ridge system, which became the locus of ridge subduction beneath continental Antarctica (Mayes et al., 1990; McCarron and Larter, 1998; Eagles et al., 2004). Although details vary between studies, there appears to be a consensus that the Bellinghausen plate ceased to move independently in Early Paleocene time (~60 Ma), having been transferred to the Pacific and Antarctic plates during a basin-wide plate reorganization event at that time (Mayes et al., 1990; Eagles et al., 2004).

The magnetic anomaly dataset requires a Farallon–Phoenix–South America triple junction throughout the Paleogene, but fails to fully constrain the configuration and paleo-geography of the Farallon–Phoenix spreading-ridge system, including its latitudinal position at the South American trench (Mayes et al., 1990; Ramos and Kay, 1992; McCarron and Larter, 1998; Eagles et al., 2004). Therefore, the shape, position and orientation of the sub-South American slab window cannot be kinematically-defined through this interval (Fig. 1), although geochemical and structural evidence favour a southerly, Patagonian position for it by Eocene time (Espinoza et al. (2005). To the south, the Antarctic–Phoenix spreading-ridge junction with the Antarctic trench is constrained (Mayes et al., 1990), but the paleo-geometry of the previously-subducted sections of the ridge, and thus the shape of the subducted slab edges, is uncertain (Fig. 1). As previously identified by Hole et al. (1991), the Antarctic slab window developed following subduction of a single plate (Phoenix), with the other plate (oceanic Antarctic) remaining fixed to the continent at the trench. Other relevant tectonic events for this interval relate to the connectivity of the Patagonian and Antarctic Peninsulas. The opening of the Drake Passage between the two overriding plates occurred not later than the Early Oligocene (ca. 31 Ma; Lawver and Gahagan, 2003), and possibly as early as Middle Eocene as suggested by micro-basin development in the adjacent precursor to the Scotia Basin (Eagles et al., 2006).

The Neogene magnetic anomaly dataset becomes increasingly robust, such that by Early Miocene time, plate boundaries and relative plate motions for the Nazca, Antarctic, Phoenix, and South American plates are well established (e.g., Shaw and Cande, 1990; Royer and Chang, 1991; Larter and Barker, 1991; Lawver et al., 1995; Tebbens and Cande, 1997; Eagles, 2003; Eagles et al., 2004). Recognition of an Early Miocene breakup of the Farallon plate into the Nazca and Cocos plates (e.g., Hey, 1977; Lonsdale, 2005) led to renaming of the northerly slab (of our study region, Fig. 1) subducting beneath Patagonia as the Nazca slab, rather than the Farallon slab, from that time forward. By 20 Ma, the Nazca–Phoenix–Antarctic oceanic triple junction was within 400 km of the South American trench and migrating towards it, with the Nazca–Phoenix spreading-ridge system having a geographically constrained configuration, and its triple junction with South America situated in the vicinity of the southern Patagonia Peninsula

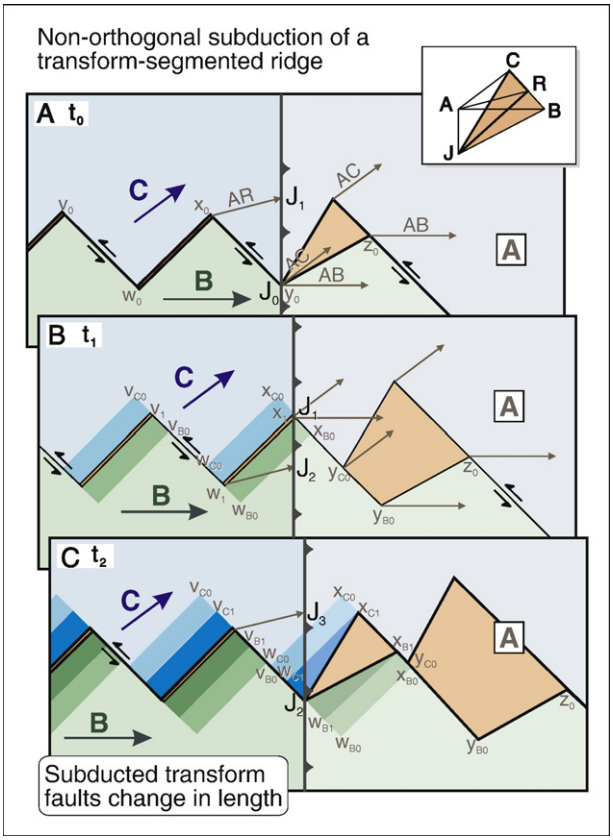

Fig. 2. Geometric method of reconstructing subsurface slab edge geometries from kinematic (plate-rotation pole) dataset in velocity space (modified from Fig. Thorkelson, 1996). This figure demonstrates how points on a slab edge can be tracked from their position in the trench in frame (A) to subsequent times (B, C) in velocity space using the relative motion vector of each oceanic plate relative to a fixed overriding plate. Because the slab edge experiences zero growth after passing through the trench, this time-tracking of velocity-space vectors maps out the edge of the slab over time. The method accurately accounts for transform-faulted slab edge shortening and lengthening which occurs during the subduction of a transform fault segment of the ridge. See text for explanation, or Thorkelson (1996) for detailed discussion.

(Mayes et al., 1990; Lawver et al., 1995). By Late Miocene time, the Nazca–Antarctic spreading-ridge system was subducting beneath Patagonia (Cande and Leslie, 1986) and the west side of the Phoenix–Antarctic spreading-ridge system was subducting beneath the Antarctic Peninsula (Hole et al., 1991; Hole and Larter, 1993; Eagles, 2003). Although not specifically highlighted in the literature, a natural outcome of the foregoing configuration of plates, coupled with Antarctica's slow convergence relative to South America (Barker, 1982), requires that the eastern end of the Phoenix–Antarctic spreading-ridge also be subducting beneath southernmost Patagonia. Phoenix–Antarctic spreading ceased at 3.3 Ma (Livermore et al., 2000; Eagles, 2003); the Nazca–Antarctic spreading-ridge system remains as the only currently subducting ridge in the region. The fate of the subducted portions of the Phoenix plate beneath both Patagonia on its east side and Antarctica on its south side is not known; one or both portions of the slabs may have foundered, or may remain at depth, attached to the fossil Phoenix oceanic crust which was captured by and is now moving with the Antarctic plate.

3. Kinematic reconstruction of Neogene slab window geometry

3.1. Method

The shape of a specific slab window can be forward-modeled following the detailed geometric methods described in Thorkelson (1996), if both the relative plate motions and plate paleo-boundaries at a selected start-time for the model are known (e.g., Breitsprecher et al., 2003; Madsen et al., 2006) or assumed (Johnston and Thorkelson, 1997). Figure 2 (modified from Fig. 4, Thorkelson, 1996) provides a summary of relevant aspects of the reconstructive methodology in velocity space for the case under study (i.e., the Chile Rise and the Phoenix–Antarctic spreading-ridge), in which transform–offset ridge segments are subducted at an oblique angle to the trench. Starting with known plate boundary geometries, all segments of a ridge system are shifted by the vector representing the relative motion for each of the diverging plates for one increment of time (1 m.y. for convenience), relative to a fixed overriding plate. Outboard of the trench (on the ocean floor), the gap between the plate edges after one increment of time is filled by growth of the slab edges along the divergent margin, and the new spreading-ridge lies midway between the shifted boundaries of the former plate edges (Fig. 2B). Inboard of the trench (beneath the overriding plate), the shape of the gap between the diverging plates (the slab window) beneath the forearc can be realized by projecting a line from the point on each slab formerly at the ridge–trench triple junction (point J_0, Fig. 2A) to the new location of the triple junction (J_1, Fig. 2B). Farther inboard, definition of the slab edges requires repetition of this procedure through multiple increments of time. Refinement of the surface projection of the slab window can then be made using known or assumed angles of slab dip, and other details as applicable, such as formation of micro-plates (e.g., Dickinson, 1997).

The specific geometric method applied is critical towards accurately reproducing the slab edge geometries, because it incorporates and accurately reconstructs the phenomenon of transformed-edge lengthening and shortening on the leading and trailing plates respectively, which results from oblique subduction of a transform–offset ridge system (Fig. 2; see also Fig. 4 in Thorkelson, 1996). This phenomenon is best described in the context that transform faults in the spreading-ridge system retain their length over time only because of equal growth on both of the plates which the fault separates. During

Table 1
Velocity-space vectors used to model the geometry of subducted slab edges from 20 Ma to present

	Stage (chron)	C6 to C5C	C5C to C5A	C5A to C5	C5 to C4A	C4A to C4	C4 to C3A	C3A to C3	C3 to C2A	C2A to C2	C2 onwards
	Interval (Ma)	~20–16 Ma	~16–12 Ma	~12–11 Ma	~11–9 Ma	~9–8 Ma	~8–7 Ma	~7–5 Ma	~5–4 Ma	~4–3 Ma	~3–0 Ma
Nazca–Phoenix–South America junction	Calculated at: Naz to fixed SAm Speed Azimuth Pho to fixed SAm Speed Azimuth	56°S 68°W 143 km/m.y. 077° 103 km/m.y. 112°									
Nazca–Antarctic–South America junction	Calculated at: Naz to fixed SAm Speed Azimuth Ant to fixed SAm Speed Azimuth		54°S 70°W 103 km/m.y. 082° 31 km/m.y. 108°	All as previous interval	48°S 72°W 93 km/m.y. 078° 15 km/m.y. 101°	All as previous interval	All as previous interval	All as previous interval	All as previous interval	48°S 72°W 79 km/m.y. 079° As previous interval	46°S 72°W 75 km/m.y. 077° 16 km/m.y. 100°
Antarctic–Phoenix–South America junction	Calculated at: Pho to fixed SAm Speed Azimuth Ant to fixed SAm Speed Azimuth		56°S 68°W 110 km/m.y. 116° 30 km/m.y. 107°	56°S 66°W 80 km/m.y. 120° As previous interval	56°S 66°W 90 km/m.y. 119° 13 km/m.y. 103°	57°S 65°W 79 km/m.y. 118° 13 km/m.y. 104°	57°S 62°W 65 km/m.y. 118° As previous interval	57°S 62°W 52 km/m.y. 121° As previous interval	57°S 62°W 41 km/m.y. 119° As previous interval	Phoenix extinct at 3.55 Ma	
Phoenix–Antarctic junction	Calculated at: Pho to fixed SAm Speed Azimuth Ant to fixed SAm Speed Azimuth	65°S 75°W 100 km/m.y. 115° 25 km/m.y. 113°	62°S 65°W 88 km/m.y. 127° 27 km/m.y. 108°	62°S 62°W 68 km/m.y. 128° 11 km/m.y. 106°	62°S 62°W 74 km/m.y. 130° As previous interval	62°S 60°W 66 km/m.y. 125° As previous interval	62°S 60°W 51 km/m.y. 131° As previous interval	61°S 58°W 48 km/m.y. 127° 12 km/m.y. 105°	61°S 58°W 36 km/m.y. 129° As previous interval		

Vectors shown are calculated proximal to approximate paleo-positions of relevant triple junctions from forward-stage rotation poles to a fixed South America, following the procedures set out in Cox and Hart (1986). Forward-stage poles used in the calculation were derived from finite-rotation poles using University of Texas online "Adder" program (Scotese and Royer, 2003). Sources of finite-rotation poles are: 1) Phoenix–Antarctic: from Eagles (2003) from ~15 Ma to present, and interpolated between that of Eagles et al. (2004) and Larter and Barker (1991) from 20–15 Ma; 2) Nazca–Antarctic: from Tebbens and Cande (1997); 3) Antarctica–South America: added from South America–Africa (Shaw and Cande, 1990) and Antarctica–Africa (Royer and Chang, 1991).

the subduction of a transform fault at orthogonal to oblique angles to the trench, plate growth is transferred to the leading-plate edge at the expense of the trailing plate (Thorkelson, 1996). In detail, the leading plate ("B" in Fig. 2) continues to grow in the ridge segment approaching or at the trench (w_0–x_0, Fig. 2A) to add one interval of plate accretion at the ridge on the inboard-facing side of the transform fault (area bounded by w_1–w_{B0}–x_{B0}–x_1, Fig. 2B). The jog in the slab edge thus grows, because there is a lack of equivalent, compensatory plate growth along the former ridge segment (y_{B0}–z_0, Fig. 2B) in the slab window (i.e. distance x_1–y_{B0} > distance v_1–w_1, Fig. 2B). Meanwhile, the trailing plate ("C" in Fig. 2) experiences the opposite phenomenon, in that newly accreted material outboard of the trench (area bounded by w_1–w_{C0}–x_{C0}–x_1, Fig. 2B) occurs on the outboard-facing side of the transform fault, where it is balanced by growth on the leading plate,

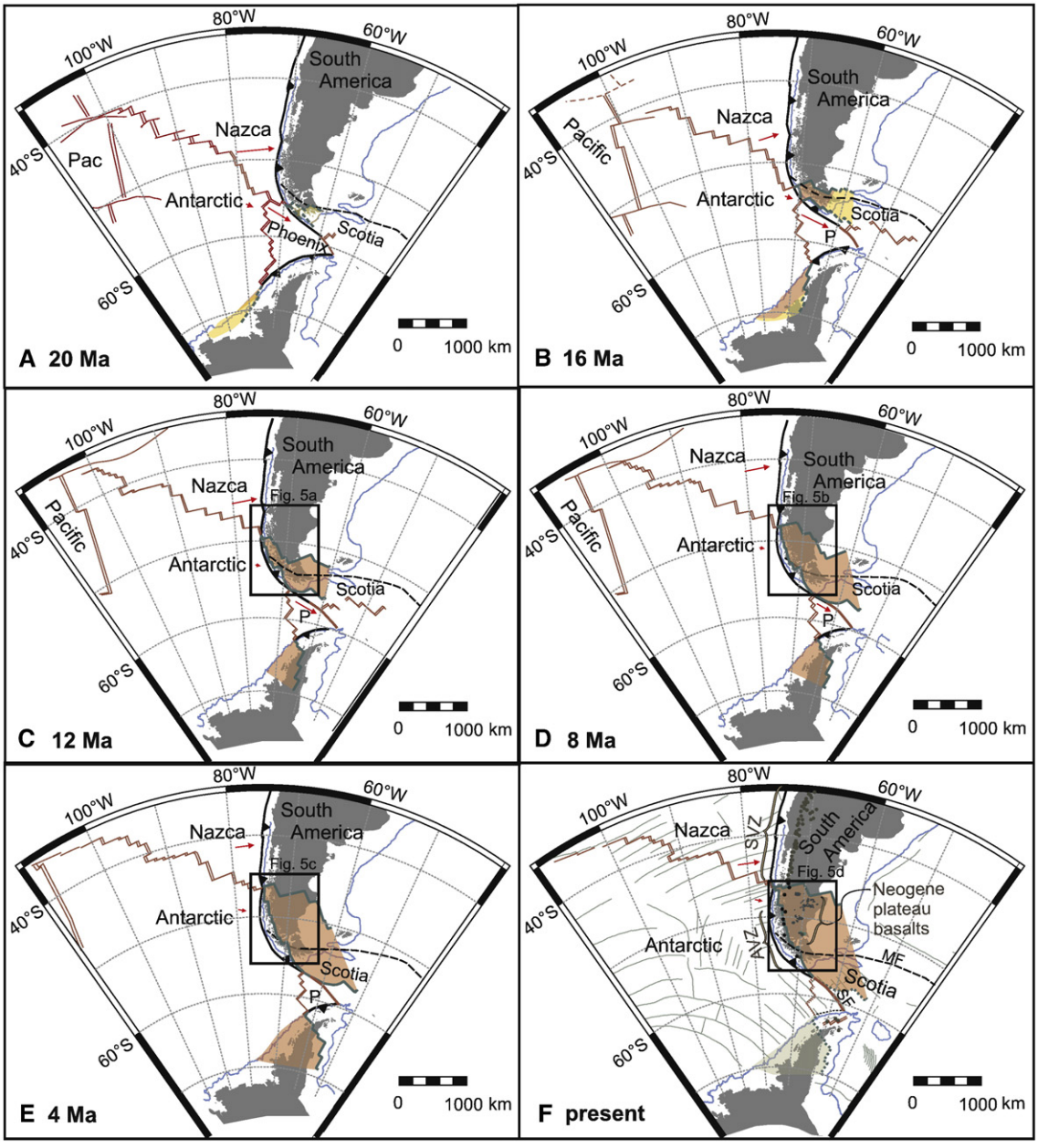

Fig. 3. Neogene kinematic evolution of the Patagonia and Antarctic slab windows. Slab window geometries (this study) are shown with their 20 Ma (A), 16 Ma (B), 12 Ma (C), 8 Ma (D), 4 Ma (E) and present-day (F) configurations. Slab window geometries are modeled using calculated velocity-space vectors provided in Table 1 (South American plate held fixed), and following the geometric methods summarized herein (see Fig. 2) and detailed in Thorkelson (1996). In the earliest frames (A and B), the geometries shown are subject to uncertainties deriving from unknown (assumed) paleo-configuration of the Nazca–Antarctic and Antarctic–Phoenix spreading-ridge systems. The portions of the slab windows subject to this assumption in input parameters are shown with dashed outline and yellow shading, versus solid lines and red shading for fully constrained, kinematically-defined portions of the slab windows. Present-day Phoenix plate edges, which may no longer exist in the subsurface in the unknown case that this slab has already foundered, are shown with dotted outline. Slab geometries are shown dip-corrected, relative to their surface projection onto overriding plate. Red arrows indicate the relative displacement for each subducting plate, holding the South American plate fixed, from each figure panel to the time of the next figure panel (4 m.y. interval). Oceanic spreading-ridge systems (solid red lines) and the relative positions and orientations of the continental landmasses are from previously published studies (Lawver et al., 1995; Tebbens and Cande, 1997; Barker, 2001). Geometries of individual landmasses (grey shading) and continental shelves (blue lines) are shown for geographic reference as at present-day in all frames; no attempt is made to correct for intra-plate crustal deformation or variations in shelf bathymetry over time. Present-day oceanic fracture zones are shown in grey (from Wessel and Smith (2006) "GMT", online mapping tool). See text for further discussion. Abbreviations: AVZ = Austral Volcanic Zone; MF = Magallanes–Fagnano Fault; P = Phoenix; SF = Shackleton Fault; SVZ = Southern Volcanic Zone. (For interpretation of the references to colour in this figure legend, the reader is referred to the web version of this article.)

and the inboard-facing, subducted portion of the transform fault (x_1–y_{C0}, Fig. 2B) experiences zero growth for overall shortening (i.e. distance x_1–y_{C0}<distance v_1–w_1, Fig. 2B). Lengthening and shortening of the subducted transform fault slab edges ceases upon commencement of subduction of the next spreading-ridge segment (i.e. distance x_{B1}–y_{B0}, Fig. 2C = distance x_1–y_{B0}, Fig. 2B). The Mendocino transform fault, at the northern edge of the California slab window, is an extreme case of differential growth/shrinkage of a subducting transform fault. As the Mendocino transform subducts, its entire length is transferred to the leading plate (the Juan de Fuca plate), leaving the trailing plate (the Pacific plate) without any offset whatsoever (e.g., Dickinson, 1997; Wilson et al., 2005).

We apply the following parameters to construct the slab window shapes and positions according to the method summarized above (Thorkelson, 1996), which is mainly based on an understanding of ridge–transform configuration, relative plate motions, and slab dip angle. In the southeast Pacific region, the specific plate motions of involved plates (Nazca, Phoenix, Antarctic, South America) relative to one another are derived (Table 1) from a robust dataset of published finite-rotation poles (Shaw and Cande, 1990; Royer and Chang, 1991; Larter and Barker, 1991; Tebbens and Cande, 1997; Eagles, 2003; Eagles et al., 2004). The paleo-geography of regional intra-plate boundaries is available at 20 Ma (Lawver et al., 1995; Tebbens and Cande, 1997; Barker, 2001), which we use as the 'start-time' for our model (Fig. 3A). Plate boundaries are re-positioned at 1 m.y. increments by a vector representing the relative motion of all points on a specific plate boundary to South America (Table 1), which we hold fixed in our model. Each oceanic spreading-ridge system is adjusted such that for each new increment in time, the ridge system is positioned midway between the departing plate edges after shifting each plate boundary by its relative-to-South America velocity-space vector (Table 1). Inboard of the trench, the shape of the subducted slab edges of the Nazca, Phoenix and Antarctic slabs are also reconstructed at 1 m.y. increments, according to the geometric procedures for determining slab window shape summarized above and set out in detail in Thorkelson (1996). Each slab edge is dip-corrected so that the plan view shown in the figure is a true surface projection relative to the horizontal, overriding plate. The Nazca slab is corrected to its present-day dip as determined from seismic data (Jarrard, 1986): 13° at shallow levels, 16° at intermediate levels, and 30° below 150 km. The Antarctic slab below Patagonia is corrected to its present-day dip of 10° (Rubio et al., 2000). The Phoenix plate is unconstrained with respect to dip, thus we have dip-corrected the dominant (southern) slab edge to an intermediate but arbitrary dip of 35°, and the minor (eastern) slab edge to an arbitrary dip of 10°, similar to the known behaviour of the Antarctic plate to its north along that same trench. The absolute motion of South America, which our modeling holds fixed, is corrected with respect to latitude–longitudes shown in Fig. 3 by keying oceanic plate boundaries of our forward-model to documented paleo-geographic positions of the Nazca–Antarctic ridge system at the times for which that feature is geographically constrained (20, 16, 11, and 4 Ma: Tebbens and Cande, 1997). The modeling of slab window geometry is undertaken in orthogonal space (Thorkelson, 1996); therefore, we have chosen a polar-stereographic map projection to eliminate errors due to non-equal-area map projections which become exaggerated at sub-polar regions under alternative projections (e.g., Mercator). We hold the Magallanes block fixed to South America (Option 2, Eagles et al., 2005).

4. Results

The kinematically-defined geometries of the Patagonian and Antarctic slab windows are presented at Fig. 3 for selected times. These geometries are shown without addressing the process of thermal erosion, i.e., the slab edges represent idealized geometries assuming they have not yet been eaten-away by anatexis, ductility increase, and disaggregation caused by heating and shearing as the slabs pass through the mantle (cf., Dickinson and Snyder, 1979; Severinghaus and Atwater, 1990; Thorkelson and Breitsprecher, 2005). Thermal erosion of the Antarctic and Patagonian slab window margins is beyond the scope of this paper because the conceptual framework for complex patterns of slab melt zonation in the case under study, namely ridge systems which are offset by transform faults, is not yet established (see Thorkelson and Breitsprecher (2005) for theoretical slab melt zonation framework applicable to simplified cases). The topic will be developed and applied to the Patagonian case in a subsequent manuscript.

Prior to Early Miocene time (e.g., Fig. 1), the shapes and positions of both the Patagonian and Antarctic slab windows are unconstrained by ocean floor kinematics because of an absence of relevant sea-floor magnetic stripes. By 20 Ma (Fig. 3A), the slab windows are beginning

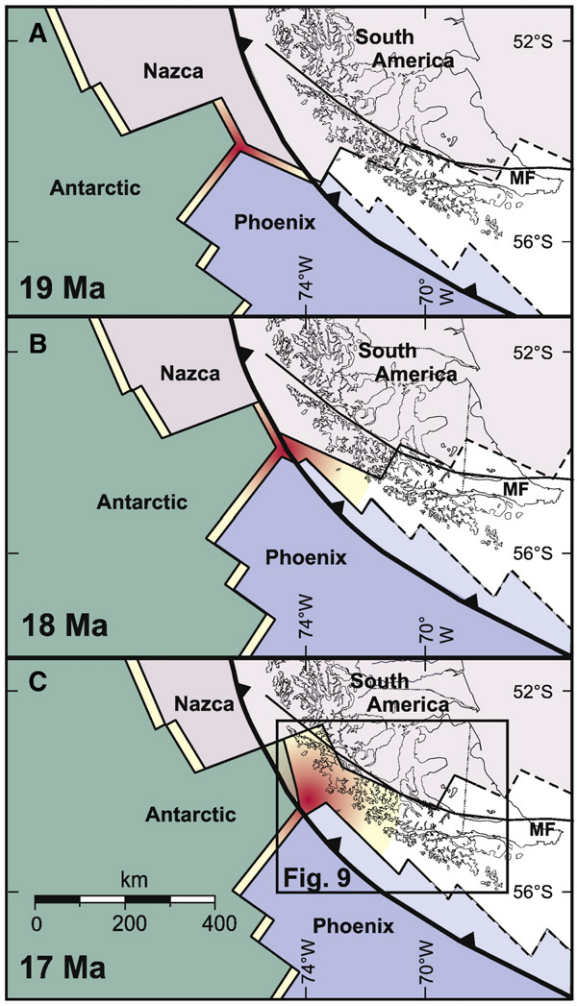

Fig. 4. Early Miocene unstable quadruple-junction event, Phoenix–Nazca–Antarctic–South American plates. Unusually high heat-flow conditions are implied for this rare and previously undocumented tectonic setting, wherein an oceanic ridge–ridge–ridge triple junction collides with a trench. High heat-flow conditions typically associated with ridge subduction (e.g. DeLong et al., 1979) are shown in pale yellow. Numerical models predict super-elevated thermal conditions and mantle upwelling within the spreading-ridge system within a 200 km radius of the oceanic triple junction (e.g. Georgen and Lin, 2002); this additional heat is shown in red. All input parameters of the modeled geometry, which holds South America fixed, are as for Fig. 3. As for early (20 Ma, 16 Ma) frames of Fig. 3, the portions of the modeled slab edges which are subject to uncertainty deriving from unconstrained Farallon–Phoenix boundary conditions are shown with dashed line. Abbreviation: MF = Magallanes–Fagnano Fault. (For interpretation of the references to colour in this figure legend, the reader is referred to the web version of this article.)

to become constrained beneath the forearc regions; their extensions beneath more inboard regions are based on the assumption that the configuration and kinematics of the subducting ridges were similar in the preceding few m.y. The Nazca–Antarctic–Phoenix oceanic triple junction is located offshore of Patagonia from 20–19 Ma, but begins to enter the trench by 18 Ma (Fig. 4A,B). At this time, four plates (Nazca, Antarctic, Phoenix and South America) share a common point of intersection, a *trench–ridge–ridge–trench quadruple junction* in the context of conventional 2-dimensional junction terminology (e.g. Kearey and Vine, 1996). By 17 Ma, the former oceanic triple junction is entirely inboard of the trench, and all 3 plates of the former ridge–ridge–ridge oceanic triple junction are actively subducting beneath South America (Fig. 4C). The trench–ridge–ridge–trench quadruple junction has been replaced by a pair of trench–ridge–trench triple junctions, and therefore the quadruple-junction condition must be classified as unstable.

By 16 Ma (Fig. 3B), the Nazca–Antarctic–Phoenix oceanic triple junction has been fully subducted. The new configuration yields an unusually shaped composite slab window, where the spreading-ridge systems of the trailing arms of the oceanic triple junction produce a doubly-pinned slab window geometry. The two new trench–ridge–trench junctions, namely the Nazca–Antarctic–South America and

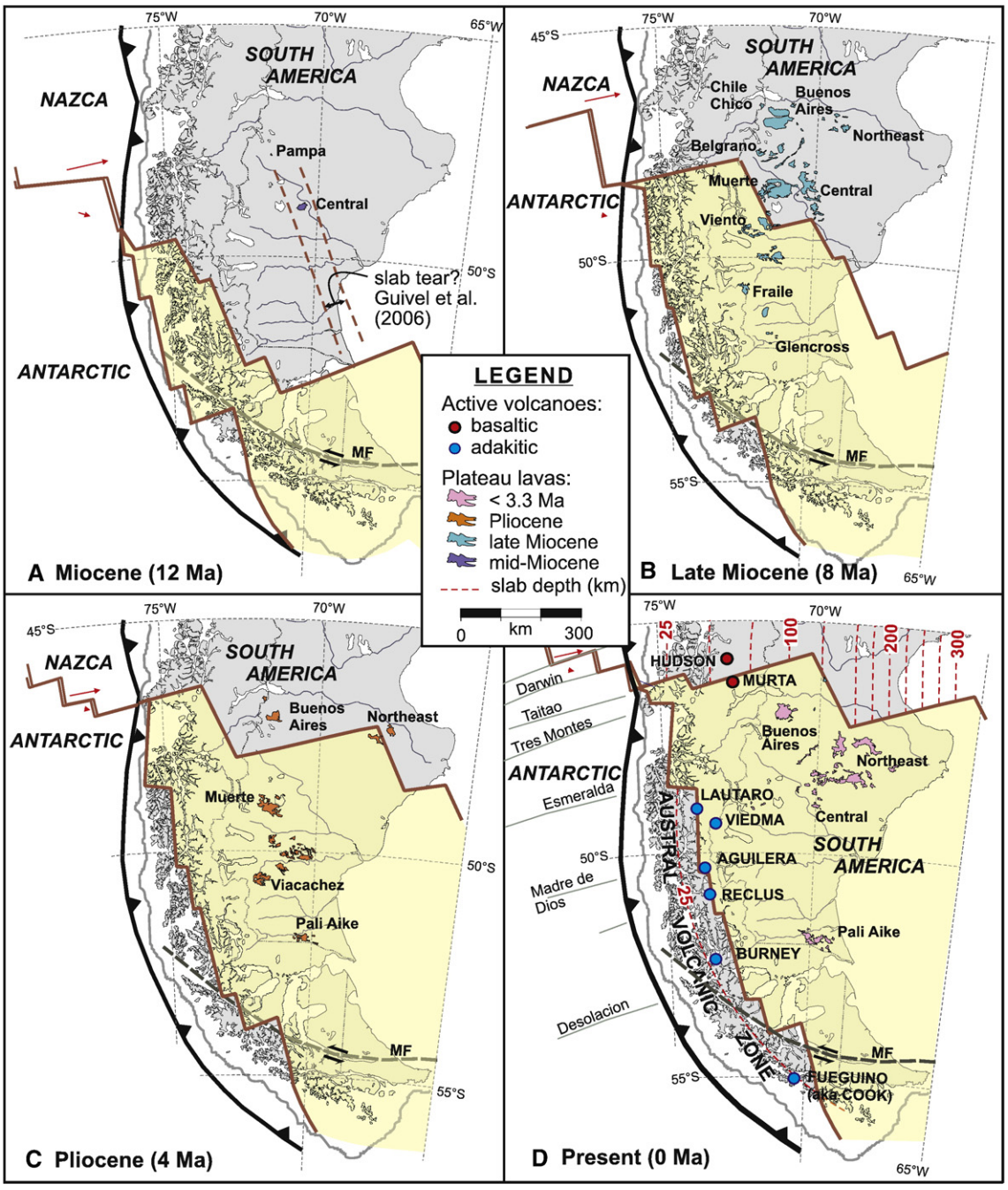

Fig. 5. Maximum extent of the Patagonia slab window through the Neogene. A) Middle–Late Miocene (12 Ma); B) Latest Miocene (8 Ma); C) Pliocene (4 Ma); D) Recent (0 Ma). The heavy lines are the kinematically-defined slab edges, and represent the maximum extent of the slabs in the subsurface prior to their reduction by thermal erosion. Red arrows indicate the relative displacement of each subducting plate, per m.y., at the time shown for each figure panel, relative to a fixed South America. Red dashed lines represent present-day depth contours to tops of slabs, simplified from published slab dip angles (see text for sources). See text for discussion. Magmatic centers from Stern and Kilian (1996), Panza et al. (2002). Base-map features generated using "GMT" program of Wessel and Smith (2006). Abbreviations used: MF = Magallanes–Fagnano Fault. (For interpretation of the references to colour in this figure legend, the reader is referred to the web version of this article.)

Antarctic–Phoenix–South America junctions, migrate away from each other north and south respectively, along the trench. The geometry at the northern margin of the Patagonian slab window, controlled by Nazca–Antarctic ridge subduction, is a rapidly-widening, south–southeast opening gap because of the large differences in convergence speed between the Nazca and Antarctic plates relative to South America (Table 1), and because of the near-parallel convergence angle of that spreading-ridge system relative to the trench. The geometry of the southern margin of the slab window, controlled by Antarctic–Phoenix ridge subduction, is that of a slowly-widening, very wide-angle, eastward-opening gap, because the convergence angle of the Phoenix plate to the South American trench is so highly oblique as to be nearly transform in orientation.

The segment of the Nazca–Antarctic spreading-ridge between the Esmeralda and Desolacion transform faults begins to subduct at 13 Ma and is fully inboard of the trench by 12 Ma (Figs. 3C, 5A). This interval also marks the onset of backarc volcanism, including ca. 12.1 Ma (K–Ar, whole rock: Ramos et al., 1991) adakitic lavas of Cerro Pampa (Kay et al., 1993) and the oldest alkali basalts at Meseta Muerte (Ar–Ar, whole rock: Gorring et al., 1997). The northernmost boundary of the 12 Ma slab window (Fig. 5A) boundary compares well with the latitude of these lavas (e.g. Guivel et al., 2006). However, the Nazca slab edge is approximately 200 km too far west of them to appeal to vertical upflow of mantle through the slab window as the cause of magmatism. Their extrusion cannot therefore be attributed to vertical migration through the slab window, and an appeal to a tear in the Nazca slab as a mechanism for triggering mafic magmatism, as proposed by Guivel et al. (2006), continues to be a viable scenario. In the forearc region, the subduction of this portion of the Chile Rise and ensuing opening of the slab window (Fig. 5C) somewhat post-dates plutonism and thermal resetting as evidenced by ca. 17–14 Ma zircon and apatite fission-track ages from plutons at Lat. 50°S (Thomson et al., 2001).

By 8 Ma, the northerly portion of the slab window has widened considerably such that it underlies much of the Patagonian Peninsula at that more northerly latitude, and is favourably situated directly beneath or adjacent to the main sequence of basaltic, asthenospherically derived late Miocene plateau lavas (Glencross, Cerro del Fraile, Meseta del Viento, Meseta de la Muerte, Meseta Central) (Figs. 3D, 5B). However, as in the preceding timeslice, the slab window remains too far west of the most northerly (Meseta del Lago Buenos Aires) and easterly (Northeast Region) plateau lavas (e.g., Gorring et al., 1997; D'Orazio et al., 2001; Brown et al., 2004) for an appeal solely to vertical upflow through it (Guivel et al., 2006).

By the end of the 8–4 Ma interval, the Nazca slab edge has migrated beyond the eastern side of the Patagonian Peninsula, and all backarc basaltic plateau lavas of this interval, except for the ca. 6–8 Ma lavas of Meseta del Lago Buenos Aires, are favourably situated directly above the slab window (Pali Aike, Meseta las Viachez, Meseta Muerte, Northeast Region) (Figs. 3E, 5C) (e.g. Gorring et al., 1997; D'Orazio et al., 2000; Gorring and Kay, 2001; Brown et al., 2004; Guivel et al., 2006). To the south, the Phoenix plate is at this time in its last stages of independent motion (Fig. 3E), with fusion to the Antarctic plate occurring at 3.3 Ma (Livermore et al., 2000).

Presently, the slab window is situated beneath all occurrences of Pleistocene to Quaternary basaltic backarc magmatism (Figs. 3F, 5D) (e.g. Stern et al., 1990; D'Orazio et al., 2000; Gorring et al., 2003; Brown et al., 2004; Guivel et al., 2006). The Rio Murta and Cerro Hudson volcanic centers, which are situated just south and north of the kinematically-defined edge of the Nazca slab respectively (Fig. 5D), have geochemical signatures requiring, amongst other components, upwelling of sub-slab depleted mantle or melts thereof associated with the Chile Rise spreading center (Demant et al., 1998; Gutierréz et al., 2005). To the south, the modeled edge of the Antarctic slab lies just inboard of adakitic (slab melt) volcanoes of the Austral Volcanic Zone (Stern et al., 1984; Stern and Kilian, 1996; Sigmarsson et al., 1998).

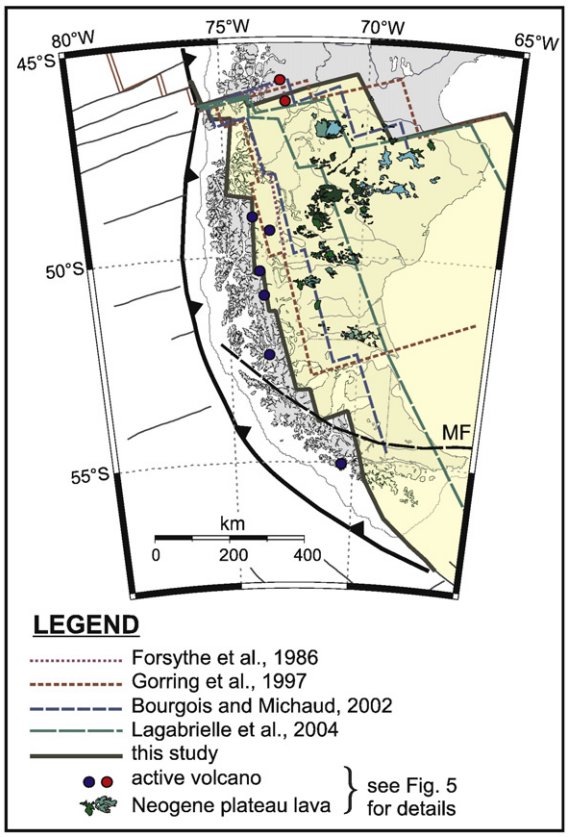

Fig. 6. Comparison of kinematically modeled modern Patagonian slab window geometry (this study) to previously published approximations of same. The new model tracks the transfer of slab edge growth from trailing to leading-plate edges during transform fault subduction (e.g. Thorkelson, 1996), resulting in a wider slab window, and a more westerly position for the Antarctic slab edge than previously estimated. Abbreviations used: MF = Magallanes–Fagnano Fault.

The present-day extent of the Patagonian slab window (Fig. 5D) is compared to previously published approximated geometries in Fig. 6. The slab window is wider than earlier approximations, which failed to take into account the lengthening of leading-plate (Nazca) transform segments and shortening of trailing-plate (Antarctic) transform segments which occurs in cases of non-orthogonal ridge subduction (Fig. 2) (Thorkelson, 1996). Specifically, the Antarctic slab edge is situated at a much more trench-ward position than any of the previous approximations; from as little as 100 km (Gorring et al., 1997) to 300 km (Lagabrielle et al., 2004) farther west. The Antarctic slab stub as defined by the kinematic model presented herein is shallow; its deepest point, the southerly triangular segment straddling the Magallanes–Fagnano transform fault, is approximately 45 km below the surface (Fig. 5D).

5. Discussion

Our treatment of ridge subduction in the southeastern Pacific basin provides an integrated view of plate divergence and convergence that led to synchronous slab window formation beneath Patagonia and the Antarctic Peninsula. Both slab windows led to changes in the physical, thermal and chemical conditions in the mantle environment, as indicated by the varied but generally non-arc-like character of Neogene magmatism (Forsythe et al., 1986; Hole et al., 1991; Kay et al., 1993; Hole and Larter, 1993; Gorring et al., 1997; D'Orazio et al., 2001; Gorring and Kay, 2001; Bourgois and Michaud, 2002; Lagabrielle et al., 2004; Espinoza et al., 2005; Guivel et al., 2006). The synchronous opening of these slab windows provided a large and

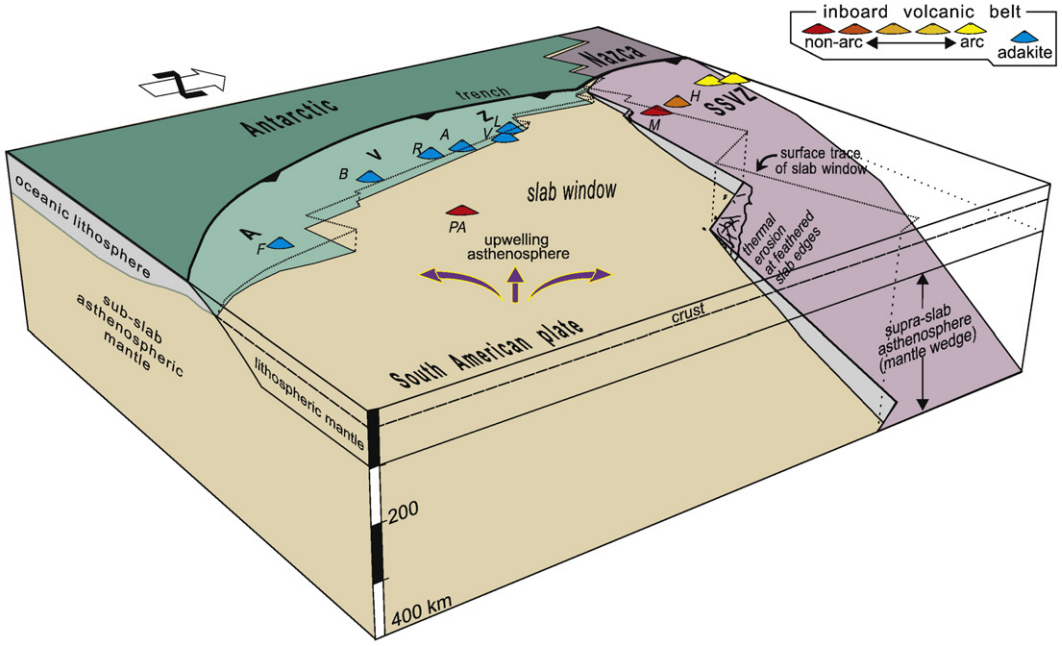

Fig. 7. Block diagram of modern Patagonia slab window. This simplified view is projected towards the northwest from a birds-eye position just northeast of the Scotia Basin. Note the shallow depth of Antarctic slab, which has not yet penetrated below typical depths for lithospheric mantle. Mantle flow is therefore unrestricted along the Antarctic slab stub, but is separated into sub- and supra-slab reservoirs by the Nazca slab. Note that feather edges of the slabs (former ridge segments) likely lose coherence following slab melting (e.g. Thorkelson and Breitsprecher, 2005) as portrayed for the Nazca slab; no attempt has been made herein to quantify the extent of slab loss to thermal erosion (see text for explanation). Abbreviations used: A = Aguilera; B = Mount Burney; F = Fueguino (aka Cook); H = Cerro Hudson; L = Lautaro; M = Rio Murta; R = Reclus; V = Viedma.

complex gap, with a combined length of over 2500 km, in an area that was previously dominated by subducting slabs (compare Fig. 1 to Fig. 3D, E, F). These slabs had separated the mantle environment into local sub-slab and supra-slab reservoirs, but their progressive removal during ridge subduction led to a broad pathway which enabled the asthenosphere to flow unimpeded both vertically and horizontally (Fig. 7).

5.1. Austral Volcanic Zone: slab anatexis versus arc magmatism

One of the outcomes of the new slab window model for Patagonia is the constraint it provides on the depth of the Antarctic slab beneath the Austral Volcanic Zone. Our calculations indicate that the maximum depth reached by the slab is 45 km, based on a slab dip angle of 10° and a commencement of Antarctic plate subduction beneath Patagonia at 17 Ma. This finding differs from previous estimates (Fig. 6) which place the leading edge of the Antarctic slab deeper and farther east. Notably, the extent of subducted Antarctic slab is significantly less than the assumed >100 km depth (e.g., Stern and Kilian, 1996) in their study of Austral Volcanic Zone magmatism (Figs. 5, 6). Despite this difference, our estimate of the extent of the Antarctic slab is compatible with the petrogenetic investigation of Stern and Kilian (1996) which concluded that the Austral Volcanic Zone was generated largely by anatexis of the subducted and metamorphosed Antarctic slab, with little or no contribution from the depleted mantle wedge (e.g., Gill, 1981; Arculus, 1994). In our construction, the Austral Volcanic Zone lies above the leading edge of the Antarctic slab with a depth of ≤45 km, where slab anatexis is likely to occur (cf. Thorkelson and Breitsprecher, 2005) but mantle anatexis is probably non-existent (e.g., Gill, 1981; Arculus, 1994). Figure 8 shows a prediction of the *future* Patagonia slab window margins, assuming present-day convergence rates and azimuth angles relative to South America, and assuming present-day slab dips, except for a slight increase to 13° for the Antarctic slab after reaching a depth of 70 km. Under these conditions, the Antarctic slab reaches minimum depths appropriate for production of mantle-derived arc magmas (~85 km) beginning at ca. −12 Ma (Fig. 8). A hypothetical chain of future arc volcanoes is shown inboard of the slab edge, where maximum melt production would occur (~95 km depth), and arc magma production would become likely at the time this depth is

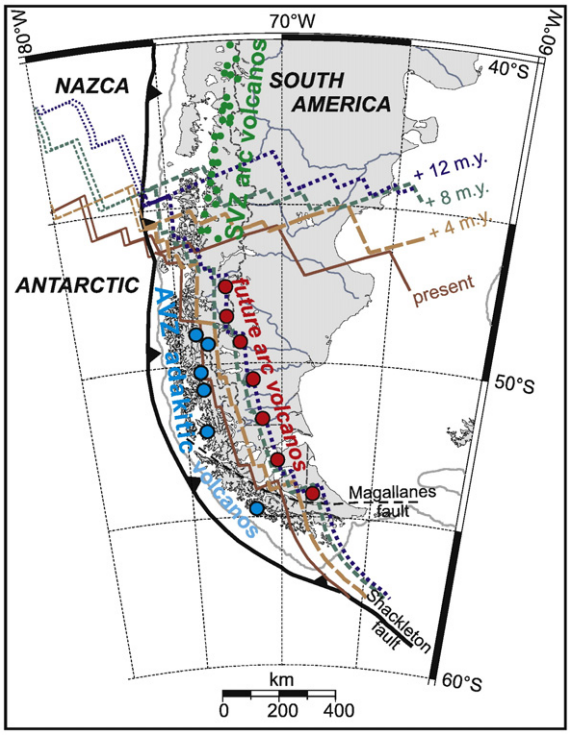

Fig. 8. Future kinematic evolution of the Patagonia slab window. The adakitic Austral Volcanic Zone is supplanted by a more easterly belt of mantle-derived arc volcanoes approximately 12–14 m.y. into the future. The future geometries shown assume constancy of present-day plate motions and further assume a minor increase in slab dip for Antarctic plate after 10 m.y. to 13°, consistent with intermediate-level dip of Nazca slab to deflect beneath South American lithosphere. Base-map features generated using "GMT" program of Wessel and Smith (2006).

achieved (~14 Ma), although the abundance of magma produced at first may be minimal due to the previous loss of volatiles during slab anatexis. However, as subduction continues, and the age of Antarctic slab entering the trench increases, slab anatexis will wane, volatiles will be carried deeper, and the Austral Volcanic Zone will be gradually replaced by a more easterly and largely mantle-derived volcanic arc.

5.2. Oceanic triple-junction subduction: long-lived thermal pulse beneath Patagonia

The subduction of the Nazca–Antarctic–Phoenix oceanic ridge–ridge–ridge triple junction has important implications for thermal conditions in the slab window starting at ca. 20 Ma, when the triple junction began approaching the trench. Such a condition, namely subduction of an oceanic triple junction, has not previously been identified in the literature and the implications must be considered in light of what is known regarding the two separate sub-conditions (ridge subduction; oceanic triple junctions) as relates to mantle flow and thermal state. At the site of a subducting spreading-ridge, heat flow in the forearc is significantly higher than elsewhere along the trench due to mantle upwelling beneath the spreading-ridge; the upwelling mantle becomes focused through the slab window in the forearc in what has been called a 'blowtorch' effect (DeLong et al., 1979; Haeussler et al., 1995; Murdie and Russo, 1999). Thermal conditions in the rest of the slab window area are also likely to be elevated (Thorkelson, 1996) because of probable mantle upwelling (e.g., Hole and Larter, 1993; cf. Johnston and Thorkelson, 1997) and an absence of the refrigerating effect of cold slab (that cools the mantle in subduction zones flanking the slab window). The thermal pulse from ridge subduction may persist for millions of years (Groome and Thorkelson, 2009-this issue). At the site of oceanic triple junctions, increased mantle upwelling and thermal flux has been modeled to be significant through a radius of ca. 200 km from the triple junction (Georgen and Lin, 2002) (Fig. 9). Consequently, subduction of the Nazca–Antarctic–Phoenix triple junction beneath Patagonia is likely to have resulted in super-elevated thermal conditions as compared documented cases of single-ridge subduction, and likely resulted in significant and persistent (cf. Heintz et al., 2005) upflow of hot asthenospheric mantle. The triggering of major mantle upflow in turn led to the long-lived and widespread outpouring of alkalic plateau basalts above and near the slab window (e.g., Gorring et al., 1997; D'Orazio et al., 2000, 2001; Guivel et al., 2006). It may also have been a causal mechanism for eastward transfer of extension in the adjacent Scotia Basin (Fig. 3A, B). Specifically, decreased spreading rates in the West Scotia Ridge are accompanied by incipient spreading at East Scotia Ridge at Chron C5C (~16.7 Ma) (Barker, 2001; Eagles et al., 2005).

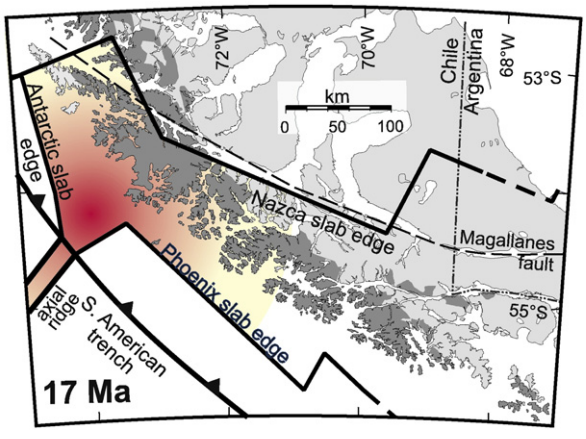

Fig. 9. High heat flow in the 17 Ma Tierra del Fuego forearc. High heat flow usually associated with ridge subduction is shown in pale yellow; super-elevated heat due to proximity of the outboard, advancing oceanic triple junction is shown in dark red. Dark-shading represents Paleogene granitoid rocks of the Seno Año Nueva phase (Patagonia Batholith), which is locally overlain by Early Miocene volcanic rocks (Hervé et al., 1984; Puig et al., 1984, Suárez et al., 1986). Light-shaded polygons represent Paleogene and older lithologies with no evidence of Miocene magmatism (Schobbenhaus and Bellizzia, 2000).

Oceanic triple junctions represent bathymetric swells in modern oceans, and the Early Miocene subduction of the Nazca–Antarctic–Phoenix junction would likely have resulted in some measure of uplift of the overriding plate. Such an effect would be expected at the locus of triple-junction subduction, which in this case occurs between Lat. 53 and 54°S, (Figs. 4, 9), and would likely continue for some unknown distance from that point towards base-level bathymetries on the subducting plates. In the Tierra del Fuego region (Fig. 9), 80 km of northward Neogene shortening (Kraemer, 2003), and easternmost transpressional faulting at ca. 24–16 Ma (Punta Gruesa fault and progressive angular unconformity, Ghiglione and Ramos, 2005), are broadly coincident with the advance of the bathymetric high of the oceanic triple junction and the coupled cell of upwelling mantle towards the trench. To the southwest, uplift in portions of the Scotia Basin beginning at 17 Ma (Eagles et al., 2005, 2006), is synchronous with the physical passage of the triple junction through the trench at ca. 18–17 Ma in the our kinematic model (Fig. 4). To the immediate north of the event (Lat. 50°S), forearc intrusions and thermal resetting are recorded between 17 and 15 Ma from fission-track studies on zircon and apatite (Thomson et al., 2001). Similarly timed onset of uplift is reported at the arc and backarc positions as far as 500 km to the north (17.1 Ma uplift at 47.5°S, apatite fission track: Haschke et al., 2006; 17–14 Ma uplift at Lat. 46–49°S, $\delta^{18}O$ and $\delta^{13}C$ evidence: Blisniuk et al., 2005). In front of the trench, the Early Miocene development of the Esmeralda and Madre de Dios Fracture Zone (Figs. 3B, 5A) (Cande and Leslie, 1986; Mayes et al., 1990) is likely also a response of the oceanic crust to instability caused by subduction of the triple junction.

6. Conclusions

The Late Cenozoic to Recent geologic history of Patagonia and the Antarctic Peninsula was dominated by ridge subduction and slab window formation that produced a slab-free region over a distance of 2500 km along the continental margins and intervening seaway. Beneath Patagonia, ridge subduction began toward the southern tip of South America giving rise to a pair of oppositely moving ridge–trench intersections. These intersections migrated both north and south, and caused the Andean magmatic arc to retreat to areas north of the growing slab window. Subduction of the Nazca–Antarctic–Phoenix triple junction beneath Patagonia at ca. 18–17 Ma led to subsequent widespread and persistent upflow of asthenospheric mantle, eruption of alkalic mafic lavas, regional uplift and possible accentuation of spreading in the Scotia plate. Pliocene to Recent descent of the Antarctic plate beneath Patagonia to depths of 25–45 km led to slab anatexis and eruption of adakitic lavas in the Austral Volcanic Zone with little input from the mantle wedge. At approximately 12 m.y. into the future, the Antarctic plate will reach depths of >85 km, leading to gradual slab-metasomatism of the mantle wedge. By −14 Ma, a new volcanic arc with a significant contribution of mafic magma will be established east of the Austral Volcanic Zone, which itself will wane as the thermal maturity of the slab increases and adakite magma production decreases.

Acknowledgements

The authors are supported by the Natural Sciences and Engineering Research Council of Canada (scholarship to KB; grant to DJT). Julianne Madsen is thanked for discussions regarding plate kinematic modeling. The manuscript benefited from a thoughtful and detailed reviews by two anonymous reviewers; Patricia McCrory is thanked for editorial duties.

References

Arculus, R.J., 1994. Aspects of magma genesis in arcs. Lithos 33, 189–298.

Barker, P.F., 1982. The Cenozoic subduction history of the Pacific margin of the Antarctic Penisnula: ridge crest–trench interactions. J. Geol. Soc. Lond. 139, 787–801.

Barker, P.F., 2001. Scotia Sea regional tectonic evolution: implications for mantle flow and palaeocirculation. Earth Sci. Rev. 55, 1–39.

Blisniuk, P.M., Stern, L.A., Chamberlain, C.P., Idleman, B., Zeitler, P.K., 2005. Climatic and ecologic changes during Miocene surface uplift in the Southern Patagonian Andes. Earth Planet. Sci. Lett. 230, 125–142.

Bourgois, J., Michaud, F., 2002. Comparison between the Chile and Mexico triple junction areas substantiates slab window development beneath northwestern Mexico during the past 12–10 Myr. Earth Planet. Sci. Lett. 201, 35–44.

Breitsprecher, K., Thorkelson, D.J., Groome, W.G., Dostal, J., 2003. Geochemical confirmation of the Kula–Farallon slab window beneath the Pacific Northwest in Eocene time. Geology 31, 351–354.

Brown, L.L., Singer, B.S., Gorring, M.L., 2004. Paleomagnetism and $^{40}Ar/^{39}Ar$ chronology of lavas from Meseta del Lago Buenos Aires, Patagonia. Geochem. Geophys. Geosyst. 5. doi:10.1029/2003GC000526.

Cande, S.C., Leslie, R.B., 1986. Late Cenozoic tectonics of the Southern Chile Trench. J. Geophys. Res. 91, 471–496.

Cole, R.B., Nelson, S.W., Layer, P.W., Oswald, P.J., 2006. Eocene volcanism above a depleted mantle slab window in southern Alaska. Geol. Soc. Am. Bull. 118, 140–158.

Cox, A., Hart, R.B., 1986. Plate Tectonics: How It Works. Blackwell, Oxford. 392 pages.

DeLong, S.E., Schwarz, W.M., Anderson, R.N., 1979. Thermal effects of ridge subduction. Earth Planet. Sci. Lett. 44, 239–246.

Demant, A., Belmar, M., Hervi, F., Pankhurst, R.J., Suarez, M., 1998. Pitrologie et giochimie des basaltes de Murta: une iruption sous-glaciaire dans les Andes patagoniennes (460 lat. S.), Chili. Relation avec la subduction de la ride du Chili. C.R. Acad. Sci. Paris. Earth Planet. Sci., 327, 795–801.

Dickinson, W.R., 1997. Tectonic implications of Cenozoic volcanism in coastal California. Geol. Soc. Am. Bull. 109, 936–954.

Dickinson, W.R., Snyder, W.S., 1979. Geometry of subducted slabs related to San Andreas Transform. J. Geol. 87, 609–927.

D'Orazio, M., Agostini, S., Innocenti, F., Haller, M.J., Manetti, P., Mazzarini, F., 2001. Slab window-related magmatism from southernmost South America; the late Miocene mafic volcanics from the Estancia Glencross area (~52°S, Argentina–Chile). Lithos 57, 67–89.

D'Orazio, M., Agostini, S., Mazzarini, F., Innocenti, F., Manetti, P., Haller, M.J., Lahsen, A., 2000. The Pali Aike Volcanic Field, Patagonia: slab-window magmatism near the tip of South America. Tectonophysics 321, 407–427.

Eagles, G., 2003. Tectonic evolution of the Antarctic–Phoenix plate system since 15 Ma. Earth Planet. Sci. Lett. 217, 97–109.

Eagles, G., Gohl, K., Larter, R.D., 2004. High-resolution animated tectonic reconstruction of the South Pacific and West Antarctic margin. Geochem. Geophys. Geosyst. 5, Q07002. doi:10.1029/2003GC00657 21 pages.

Eagles, G., Livermore, R.A., Fairhead, J.D., Morris, P., 2005. Tectonic evolution of the west Scotia sea. J. Geophys. Res. 110, 1–19.

Eagles, G., Livermore, R., Morris, P., 2006. Small basins in the Scotia Sea: the Eocene Drake Passage gateway. Earth Planet. Sci. Lett. 242, 343–353.

Espinoza, F., Morata, D., Pelleter, E., Maury, R.C., Suárez, M., Lagabrielle, Y., Polvé, M., Bellon, H., Cotton, J., De la Cruz, R., Guivel, C., 2005. Petrogenesis of the Eocene and Mio-Pliocene alkaline basaltic magmatism in Meseta Chile Chico, southern Patagonia, Chile: evidence for the participation of two slab windows. Lithos 82, 315–343.

Forsythe, R., Nelson, E., 1985. Geological manifestations of ridge collision; evidence from the Golfo de Penas–Taitao Basin, southern Chile. Tectonics 4, 477–495.

Forsythe, R.D., Nelson, E.P., Carr, M.J., Kaeding, M.E., Hervé, M., Mpodozis, C., Soffia, J.M., Harambour, S., 1986. Pliocene near-trench magmatism in southern Chile: a possible manifestation of ridge collision. Geology 14, 23–27.

Georgen, J.E., Lin, J., 2002. Three-dimensional passive flow and temperature structure beneath oceanic ridge–ridge–ridge triple junctions. Earth Planet. Sci. Lett. 204, 115–132.

Ghiglione, M.C., Ramos, V.A., 2005. Progression of deformation and sedimentation in the southernmost Andes. Tectonophysics 405, 25–46.

Gill, J.P., 1981. Orogenic Andesites and Plate Tectonics. Springer-Verlag, Berlin.

Gorring, M.L., Kay, S.M., 2001. Mantle processes and sources of Neogene slab window magmas from Southern Patagonia, Argentina. J. Petrol. 42, 1067–1094.

Gorring, M.L., Kay, S.M., Zeitler, P.K., Ramos, V.A., Rubiolo, D., Fernandez, M.L., Panza, J.L., 1997. Neogene Patagonian plateau lavas; continental magmas associated with ridge collision at the Chile triple junction. Tectonics 16, 1–17.

Gorring, M., Singer, B., Gowers, J., Kay, S.M., 2003. Plio-Pleistocene basalts from the Mesata del Lago Buenos Aires, Argentina: evidence for asthenosphere–lithosphere interactions during slab window magmatism. Chem. Geol. 193, 215–235.

Groome, W.G., Thorkelson, D.J., 2009. The three-dimensional thermo-mechanical signature of ridge subduction and slab window migration. Tectonophysics 464, 70–83 (this issue).

Groome, W.G., Thorkelson, D.J., Friedman, R.M., Mortensen, J.K., Massey, N.W.D., Marshall, D.D., Layer, P.W., 2003. Magmatic and tectonic history of the leech river complex, Vancouver island, British Columbia: evidence for ridge–trench intersection and accretion of the crescent terrane. In: Sisson, V.B., Roeske, S., Pavlis, T.L. (Eds.), Geology of a Transpressional Orogen Developed During Ridge–Trench Interaction Along the North Pacific Margin. Geol. Soc. Am. Spec. Paper, vol. 371, pp. 327–354.

Guivel, C., Lagabrielle, Y., Bourgois, J., Martin, H., Arnaud, N., Fourcade, S., Cotten, J., Maury, R.C., 2003. Shallow melting of oceanic crust during spreading ridge subduction: origin of near-trench Quaternary volcanism at the Chile Triple Junction. J. Geophys. Res 108 (B7), 2345.

Guivel, C., Morata, D., Pelleter, E., Espinoza, F., Maury, R.C., Lagabrielle, Y., Polvé, M., Bellon, H., Cotton, J., Benoit, M., Suárez, M., De la Cruz, R., 2006. Miocene to Late Quaternary Patagonian basalts (46–47°S): geochronometric and geochemical evidence for slab tearing due to active spreading ridge subduction. J. Volcanol. Geotherm. Res. 149, 346–370.

Gutierréz, F., Gioncada, A., González Ferran, O., Lahsen, A., Mazzuoli, R., 2005. The Hudson Volcano and surrounding monogenetic centers (Chilean Patagonia): an example of volcanism associated with ridge–trench collision environment. J. Volcanol. Geotherm. Res. 145, 207–233.

Haeussler, P.J., Bradley, D., Goldfarb, R., Snee, L., Taylor, C., 1995. Link between ridge subduction and gold mineralization in southern Alaska. Geology 23, 995–998.

Haeussler, P.J., Bradley, D.C., Wells, R.E., Miller, M.L., 2003. Life and death of the Resurrection plate: evidence for its existence and subduction in the northeastern Pacific in Paleocene–Eocene time. Geol. Soc. Am. Bull. 115, 867–880.

Haschke, M., Sobel, E.R., Blisniuk, P., Strecker, M.R., Warkus, F., 2006. Continental response to active ridge subduction. Geophys. Res. Lett. 33, L15315. doi:10.1029/2006GL025972.

Heintz, M., Debayle, E., Vauchez, A., 2005. Upper mantle structure of the South American continent and neighboring oceans from surface wave tomography. Tectonophysics 406, 115–139.

Hervé, M., Suárez, M., Puig, A., 1984. The Patagonian Batholith S of Tierra del Fuego, Chile: timing and tectonic implications. J. Geol. Soc. Lond. 141, 909–917.

Hey, R., 1977. Tectonic evolution of Cocos–Nazca spreading center. Geol. Soc. Am. Bull. 88, 1404–1420.

Hole, M.J., 1988. Post-subduction alkaline volcanism along the Antarctic Peninsula. J. Geol. Soc. Lond. 145, 985–998.

Hole, M.J., Larter, R.D., 1993. Trench-proximal volcanism following ridge crest–trench collision along the Antarctic Peninsula. Tectonics 12, 879–910.

Hole, M.J., Rogers, G., Saunders, A.D., Storey, M., 1991. Relation between alkalic volcanism and slab- window formation. Geology 19, 657–660.

Jarrard, R.D., 1986. Relations among subduction parameters. Rev. Geophys. 24, 217–284.

Johnson, C.M., O'Neil, J.R., 1984. Triple junction magmatism; a geochemical study of Neogene volcanic rocks in western California. Earth Planet. Sci. Lett. 71, 241–263.

Johnston, S.T., Thorkelson, D.J., 1997. Cocos–Nazca slab window beneath Central America. Earth Planet. Sci. Lett. 146, 465–474.

Kay, S.M., Ramos, V.A., Marquez, M., 1993. Evidence in Cerro Pampa volcanic rocks for slab-melting prior to ridge–trench collision in southern South America. J. Geol. 101, 703–714.

Kearey, P., Vine, F.J., 1996. Global Tectonics, (2nd Ed). Blackwell Science, Oxford. 333 p.

Kraemer, P.E., 2003. Orogenic shortening and the origin of the Patagonian orocline (56°S. Lat). J. S. Am. Earth Sci. 15, 731–748.

Lagabrielle, Y., Suárez, M., Rossello Lagabrielle, Y., Suárez, M., Rossello, E.A., Hérail, G., Martinod, J., Régnier, M., De la Cruz, R., 2004. Neogene to Quaternary tectonic evolution of the Patagonian Andes at the latitude of the Chile Triple Junction. Tectonophysics 385, 211–241.

Larter, R.D., Barker, P.F., 1991. Effects of ridge crest–trench interaction on Antarctic–Phoenix spreading: forces on a young subducting plate. J. Geophys. Res. 96, 19583–19607.

Lawver, L.A., Gahagan, L.M., 2003. Evolution of Cenozoic seaways in the circum-Antarctic region. Palaeogeog. Palaeoclim. Palaeoecol. 198, 11–37.

Lawver, L.A., Keller, R.A., Fisk, M.R., Strelin, J.A., 1995. Bransfield Strait, Antarctic Peninsula: active extension behind a dead arc. In: Taylor, B. (Ed.), Backarc Basins: Tectonics and Magmatism. Plenum, New York, pp. 315–342.

Livermore, R., Balanyá, J.C., Maldonado, A., Martinez, J.M., Rodriguez-Fernández, J., De Galdeano, C.S., Zaldivar, J.G., Jabaloy, A., Barnolas, A., Somoza, L., Hernández-Molina, J., Suriñach, E., Viseras, C., 2000. Autopsy on a dead spreading center: the Phoenix Ridge, Drake Passage, Antarctica. Geology 28, 607–610.

Lonsdale, P., 2005. Creation of the Cocos and Nazca plates by fission of the Farallon plate. Tectonophysics 404, 237–264.

Madsen, J.K., Thorkelson, D.J., Friedman, R.M., Marshall, D.D., 2006. Cenozoic to Recent plate configurations in the Pacific Basin: ridge subduction and slab window magmatism in western North America. Geosphere 2, 11–34.

Marshak, R.S., Karig, D.E., 1977. Triple junctions as a cause for anomalously near-trench igneous activity between the trench and volcanic arc. Geology 5, 233–236.

Mayes, C.L., Lawver, L.A., Sandwell, D.T., 1990. Tectonic history and new isochron chart of the South Pacific. J. Geophys. Res. 95, 8543–8567.

McCarron, J.J., Larter, R.D., 1998. Late Cretaceous to early Tertiary subduction history of the Antarctic Peninsula. J. Geol. Soc. 155, 255–268.

Murdie, R.E., Russo, R.M., 1999. Seismic anisotropy in the region of the Chile margin triple junction. J. S. Am. Earth Sci. 12, 261–270.

Panza, J.L., Sacomani, L.E., Cobos, J.C., 2002. Mapa Geológico de la Provincia de Santa Cruz, República Argentina, 1:750,000. Servicio Geológico Minero Argentino, Instituto de Geología y Recursos Minerales, Buenos Aires, Argentina.

Puig, A., Hervé, M., Suárez, M.G., Saunders, A.D., 1984. Calc-alkaline and alkaline Miocene and calc-alkaline Recent volcanism in the Southernmost Patagonian Cordillera. J. Volcanol. Geotherm. Res. 21, 149–163.

Ramos, V.A., Kay, S.M., 1992. Southern Patagonian plateau basalts and deformation: backarc testimony of ridge collision. Tectonophysics 205, 261–282.

Ramos, V.A., Kay, S.M., Marques, M., 1991. La dacita Cerro Pampa (Mioceno-Provincia de Santa Cruz, Argentina): evidencias de la colision de una dorsal oceanica. IV Congreso Geologico Chileno 2, 747–751.

Royer, J.-Y., Chang, T., 1991. Evidence for relative motions between the Indian and Australian plates during the last 20 Myr from plate tectonic reconstructions: implications for the deformation of the Indo-Australian plate. J. Geophy. Res. 96, 11799–11802.

Rubio, E., Torné, M., Vera, E., Díaz, A., 2000. Crustal structure of the southernmost Chilean margin from seismic and gravity data. Tectonophysics 323, 39–60.

Suárez, M., Puig, A., Hervé, M., 1986. K–Ar dates on granitoids from Archipielago Cabo de Hornos, southernmost Chile. Geol. Mag. 123, 581–584.
Schobbenhaus, C., Bellizzia, A., 2000. Geologic Map of South America, 1:5,000,000. Commission for the Geological Map of the World, Geological Survey of Brazil.
Scotese, C., Royer, J.Y., 2003. "Adder", On-line Software, University of Texas, Institute for Geophysics. http://www.ig.utexas.edu/research/projects/plates/programs/add_euler.htm.
Severinghaus, J., Atwater, T., 1990. Cenozoic geometry and thermal state of the subducting slabs beneath western North America. In: Wernicke, P., Brian (Eds.), Basin and Range Extensional Tectonics Near the Latitude of Las Vegas, Nevada. Memoir, vol. 176. Geological Society of America, Boulder CO, pp. 1–22.
Shaw, P.R., Cande, S.C., 1990. High-resolution inversion for South Atlantic plate kinematics using joint altimeter and magnetic anomaly data. J. Geophys. Res. 95, 2625–2644.
Sigmarsson, O., Martin, H., Knowles, J., 1998. Melting of a subducting oceanic crust from U–Th disequilibria in austral Andean lavas. Nature 394, 566–568.
Sisson, V.B., Pavlis, T.L., Roeske, S.M., Thorkelson, D.J., 2003. An overview of ridge–trench interactions in modern and ancient settings. In: Sisson, V.B., Roeske, S., Pavlis, T.L. (Eds.), Geology of a Transpressional Orogen Developed During Ridge–Trench interaction Along the North Pacific Margin. Geol. Soc. Am. Spec. Paper, vol. 371, pp. 1–18.
Staudigel, H., McCulloch, M.T., Zindler, A., Perfit, M.R., 1987. Complex ridge subduction and island arc magmatism; an isotopic study of New Georgia forearc and the Woodlark Basin. In: Taylor, B., Exon, N.F. (Eds.), Marine Geology, Geophysics and Geochemistry of the Woodlark Basin–Solomon Islands. Circum-Pacific Council for Energy and Mineral Resources. Earth Sci. Ser., vol. 7, pp. 227–240.
Stern, C.R., Kilian, R., 1996. Role of the subducted slab, mantle wedge, and continental crust in the generation of adakites from the Andean Austral Volcanic Zone. Contrib. Mineral. Petrol. 123, 263–281.
Stern, C.R., Futa, K., Muehlenbachs, K., 1984. Isotope and trace element data for orogenic andesites from the Austral Andes. In: Harmon, R.S., Barreiro, B.A. (Eds.), Andean Magmatism: Chemical and Isotopic Constraints. Shiva Publishing Limited, Chesire, U.K., pp. 31–46.
Stern, C.R., Frey, F.A., Futa, K., Zartman, R.E., Peng, Z., Kyser, T.K., 1990. Trace-element and Sr, Nd, Pb, and O isotopic composition of Pliocene and Quaternary alkali basalts of the Patagonian Plateau lavas of southernmost South America. Contrib. Mineral. Petrol. 104, 294–308.
Tebbens, S.F., Cande, S.C., 1997. Southeast Pacific tectonic evolution from early Oligocene to Present. J. Geophys. Res. 102, 12061–12084.
Thomson, S.N., Hervé, F., Stöckhert, B., 2001. Mesozoic–Cenozoic denudation history of the Patagonian Andes (southern Chile) and its correlation to different subduction processes. Tectonics, 20, 693–711.
Thorkelson, D.J., 1996. Subduction of diverging plates and the principles of slab window formation. Tectonophysics 255, 47–63.
Thorkelson, D.J., Taylor, R.P., 1989. Cordilleran slab windows. Geology 17, 833–836.
Thorkelson, D.J., Breitsprecher, K., 2005. Partial melting of slab window margins: genesis of adakitic and non-adakitic magmas. Lithos 79, 25–41.
Wessel and Smith (2006) "GMT" 4.1.3 http://gmt.soest.hawaii.edu/.
Wilson, D.S., McCrory, P.A., Stanley, R.G., 2005. Implications of volcanism in coastal California for the Neogene deformation history of western North America. Tectonics 24. doi:10.1029/2003TC001621.